

Developing Atovaquone and YM155 as Chemotherapeutic Agents against Ovarian Cancer

Amruta Priyadarshini Nayak

Department of Biology,

Indian Institute of Science, Education and Research, Pune, India

Research Mentor:

Prof. Manish Patankar

Professor, Department of Obstetrics and Gynecology

University of Wisconsin-Madison, Madison, WI, USA

Thesis Advisor:

Dr. Vineeta Bal

Visiting Faculty, Indian Institute of Science, Education and Research,

Pune, India

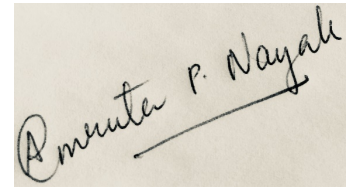


CERTIFICATE

This is to certify that this dissertation entitled *Developing Atovaquone and YM155 as Chemotherapeutic Agents Against Ovarian Cancer* towards the partial fulfilment of the BS-MS dual degree programme at the Indian Institute of Science Education and Research, Pune represents study/work carried out by Amruta Priyadarshini Nayak at Department of Obstetrics and Gynecology, University of Wisconsin-Madison, Madison, WI, USA under the supervision of Manish S. Patankar, Professor, Department of Obstetrics and Gynecology, University of Wisconsin-Madison, Madison, WI, USA during the academic year of 2017-18.



Manish S. Patankar
Professor,
University of Wisconsin-Madison,
Madison, WI, USA



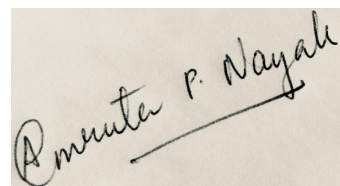
Amruta Priyadarshini Nayak
20131064
Indian Institute of Science Education and Research,
Pune, India

DECLARATION

I hereby declare that the matter embodied in the report entitled *Developing Atovaquone and YM155 as Chemotherapeutic Agents Against Ovarian Cancer* are the results of the work carried out by me at the Department of Obstetrics and Gynecology, University of Wisconsin-Madison, Madison, WI, USA, under the supervision of Prof. Manish S. Patankar and the same has not been submitted elsewhere for any other degree.



Manish S. Patankar
Professor,
University of Wisconsin-Madison,
Madison, WI, USA



Amruta Priyadarshini Nayak
20131064
Indian Institute of Science Education and Research,
Pune, India

In loving memory of my Aai, the most caring and inspirational grandmother ever.

ACKNOWLEDGEMENT

I start my acknowledgement by thanking Prof. Manish Patankar for giving me the opportunity to conduct my master's dissertation research in his lab at University of Wisconsin-Madison. Along with giving me the appointment of Undergraduate Research Assistant at the University of Wisconsin-Madison, he guided me through each and every step of this year-long research project. His insights on bringing new dimensions to the project and critically analyzing the results helped me grow as a scientist. I would like to thank Dr. Lisa Barroilhet for providing me with the funding to work in Patankar Lab. I would also like to thank Dr. Vineeta Bal for reviewing my proposal and giving me valuable inputs on experiment design and writing during my mid-year and end-of-year evaluation.

I am highly grateful to the Patankar lab members without whom this project would have been impossible. Dr. Arvinder Kapur was always there to hear my thoughts on troubleshooting the experiments and she helped me get back to work again when my experiments would not work. I would like to thank Mildred Felder for assisting me with and carrying out the mouse experiments. It would have been impossible to carry out my experiments without her facilitating the reagent purchase requests. The hours spent in the lab could not have been better without the jokes and laughter shared with Yousef, Kristal, Roberta and Samantha.

Life at Madison was made pleasant and memorable by all the warmth and support from the new friends I made here. My roommates – Kaivalya, Sripradha and Samartha helped me transition into the new lifestyle here. The weekend outings and dinners with Kanika, Akash, Apoorv and Pratyush made this year worth remembering. Last but not the least, my parents and friends back home, who were always there, just a phone call away, listened to all my worries and were pillars of support all throughout.

Amruta

ABSTRACT

Atovaquone, an FDA-approved antimalarial drug and YM155, a drug that has cleared Phase II clinical trials for lung cancer and melanoma, reduce the viability of mouse ovarian cancer cells. Both the drugs induce apoptosis in these cells by inducing oxidative stress. Simultaneously, there is also induction of autophagy and increase in the levels of Nrf-2 in the cells, likely reducing the efficacy of the drugs. Usage of inhibitors of either autophagy or Nrf2 could synergistically increase the efficacy of the drugs. Atovaquone, administered orally as Mepron, is found to be effective in decreasing the tumor burden and ascites fluid accumulation *in vivo* when murine ovarian cancer cells were intraperitoneally implanted in syngeneic C57BL/6 mice. This study, thus, lays out the foundation for further developing the atovaquone and YM155 as chemotherapeutic agents against ovarian cancer.

List of Figures

1. Figure 1: Relative estimate of new cancer-associated incidences and deaths worldwide in 2012
2. Figure 2: Classification of ovarian cancers
3. Figure 3: Chemical structure of atovaquone
4. Figure 4: Oxidative states of ubiquinone
5. Figure 5: Chemical structure of YM155
6. Figure 6: Structural comparison of atovaquone and YM155 with ubiquinone
7. Figure 7: Measurement of cell viability by MTT assay
8. Figure 8: Trends of markers of apoptosis probed by western blotting in ID8 and MOSEC cells after treatment with atovaquone
9. Figure 9: Trends of markers of apoptosis probed by western blotting in ID8 and MOSEC cells after treatment with YM155
10. Figure 10: Evaluation of apoptosis induced by atovaquone treatment using annexin-V-FITC and propidium iodide staining followed by flow cytometry
11. Figure 11: Evaluation of apoptosis induced by YM155 treatment using annexin-V-FITC and propidium iodide staining followed by flow cytometry
12. Figure 12: Evaluation of apoptosis induced by atovaquone with NAC pre-treatment using annexin-V-FITC and propidium iodide staining followed by flow cytometry
13. Figure 13: Apoptosis induced by YM155 with NAC pre-treatment using annexin-V-FITC and propidium iodide staining followed by flow cytometry
14. Figure 14: Generation of intracellular reactive oxygen species upon atovaquone and YM155 treatment.
15. Figure 15: Treatment with atovaquone or YM155 decreases expression of survivin and PCNA and increases the expression of p53.
16. Figure 16: Treatment with atovaquone or YM155 induces autophagy.
17. Figure 17: Treatment with atovaquone or YM155 increases expression of NRF-2.
18. Figure 18: Mepron
19. Figure 19: Treatment with Mepron decreases ascites accumulation reflected in weight of animal.
20. Figure 20: Treatment with Mepron decreases ascites accumulation.
21. Figure 21: Treatment with Mepron decreases tumor burden.

List of Tables

Table 1: Genetic markers associated with different types of ovarian tumors

Introduction and Background

Cancer, as a pathological condition, has been documented in science and medical journals for more than two-hundred years (DeVita and Rosenberg, 2012). The *New England Journal of Medicine* reports different strategies used by medical practitioners to handle tumors early in this period of last two-hundred years and various hypothesis proposed by some of them about the origins of the disease. Since then, there have been several advances in the field of cancer biology and medicine leading to therapies that have increased the 5-year survival rates and decreased death rates in cancer patients.

With our improved understanding, we know that the cumulative risk associated with the incidence of all types of cancers increases with age (Howlader N, et al, 2017). This is so because the major underlying cause of cancer is mutations in the genes that are essential for controlled cell growth and proliferation. Mutations are random events and the chances of oncogenes and tumor suppressor genes getting mutated increase with the age of an individual. The world has seen a population explosion in the past two centuries, thanks to medical advances and increase in the quality of life. With technological advancements and urbanization, the world has also witnessed a significant shift in lifestyles in terms of diet and behavior (WHO, 2018).

With increased life spans and 'modern' lifestyles, cancer incidence is at an all-time high. The number of reported cases of cancer increases every year and this trend is expected to continue for many decades (WHO, 2018). According to World Health Organization, there were 14 million cases reported worldwide in 2012 (Figure 1) and the number is projected to increase to 22 million in the next two decades. Cancer also has a very high death rate with nearly 8 million cancer-related deaths in 2012 (Figure 1). In India, cancer is the second most common cause of death, trailing behind cardiovascular diseases (NICPR, 2018). India is a highly populated country and as a result, the number of new incidences and deaths are also very high. In 2012, it was estimated that nearly 1 million new cases and nearly 680,000 cases of deaths due to cancer were reported in India (Figure 1). With so many lives affected worldwide, cancer has indeed become a global epidemic.

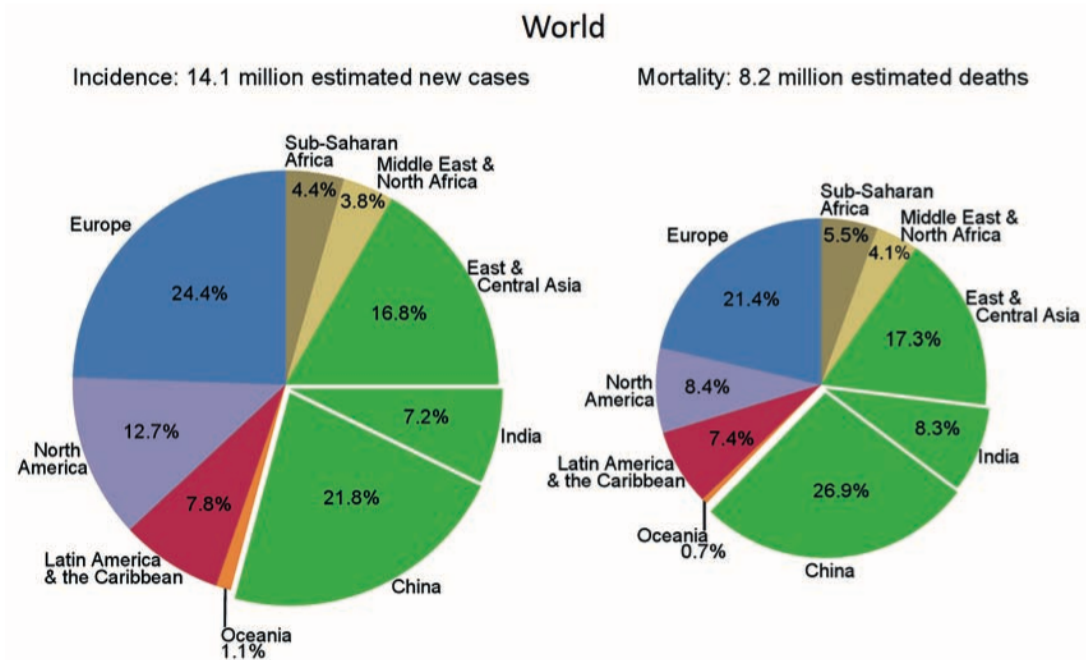


Figure 1 Relative estimate of new incidences and deaths associated with cancer by major regions of the world in 2012 (both sexes combined). Source: World Cancer Report 2014 (Stewart and Wild, 2014).

Ovarian Cancer

According to reports from the American Cancer Society, ovarian cancer is the most lethal gynecological cancer. It has the highest incidence-to-death ratio, that of 69%. This is a very high number compared to that of breast cancer for which the incidence-to-death ratio is only 19% (Siegel et al., 2017). It is estimated that in 2018, about 22000 women will receive a new diagnosis of ovarian cancer and about 14000 women will die from it in the United States (American Cancer Society, 2018). The incidence rates of ovarian cancer are highest in northern and eastern Europe, North America, and Australia, and are much lower in Africa and most of Asia. Specifically in India, in 2012, nearly 27,000 new cases and nearly 20,000 deaths were estimated to be reported due to ovarian cancer (Stewart and Wild, 2014).

The reasons behind such high lethality are multifold. First, the clinical symptoms exhibited in the early stages of ovarian cancer are not very specific and they often lead to erroneous

diagnosis. As a result, ovarian cancer is often diagnosed in advanced stages when the tumors have become aggressive and have metastasized throughout the peritoneum. At such stages, there is a high rate of relapse and the recurring tumor is resistant to most of the available treatments (Kipps et al., 2013). Second, ovarian cancer is not comprised of a single type of tumor. It is now established that ovarian cancer is a heterogeneous disease, comprising of several subtypes that originate in the female reproductive tract - each with a distinct morphological and genetic feature. Such heterogeneous presentation further complicates correct diagnosis and approaches for treatment of ovarian cancer.

Classification of Ovarian Cancers

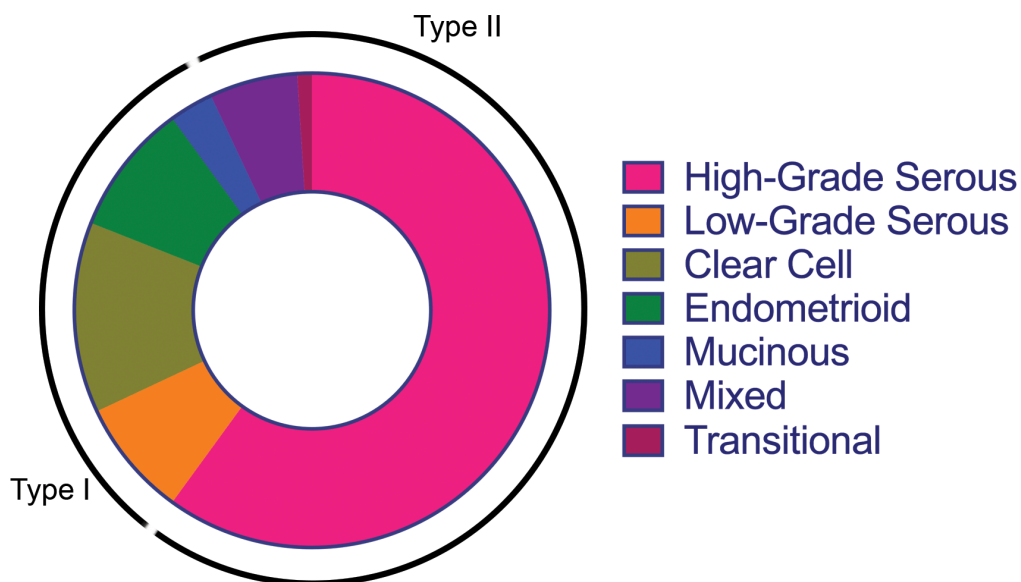


Figure 2 Classification of Ovarian Cancers. Data Source: (Seidman et al., 2004).

Based on the morphological and genetic markers, epithelial ovarian cancer is classified into Type I or II tumors. The type I tumors include low-grade serous, clear cell, endometrioid and mucinous ovarian cancer. These tumors exhibit morphological markers that are common to the parent benign neoplasms and the carcinoma they develop into, thus exhibiting a clear continuum of morphological markers.

The type II tumors include high-grade serous, mixed and transitional carcinomas. However, due to lack of distinctive morphology, all the three often get classified as high-

grade serous ovarian carcinoma. The type II tumors are often diagnosed at an advanced stage, at which these are highly aggressive.

The type I and type II tumors also vary in terms of the genetic markers they express which are listed in table 1. Another point of difference between the two types is the precursor tissues from which these arise. The type I tumors mostly arise from the benign extraneous lesions such as endometriosis that implant on the ovary and peritoneal surfaces. These benign lesions undergo malignant transformation give rise to Type I ovarian carcinoma. Such transformation also accounts for the morphological resemblance exhibited by type I tumors to the tissues of their origin. However, most type II tumors are known to develop from serous tubal intraepithelial carcinoma (STIC) in the fallopian tube. Such a development may account for their dissemination to the ovary and extraovarian sites and aggressive progression (Kurman and Shih, 2016).

Tumor type	Genetic Markers
<i>Type I tumors</i>	
Low-Grade Serous	<i>KRAS, BRAF, ERBB2</i>
Clear Cell	<i>PIK3CA</i>
Low-Grade Endometrioid	<i>CTNNB1, PTEN, PIK3CA</i>
Mucinous	<i>KRAS</i>
<i>Type II tumors</i>	
High-Grade Serous	<i>TP53, CCNE1</i>

Table 1: Genetic markers for the different types of ovarian tumors. Data Source: (Kurman and Shih, 2010)

Most of the reported cases (nearly 75%) of all ovarian cancer cases belong to type II tumors which have very similar morphological features and poor prognosis (Lengyel, 2010). As a result, ovarian cancer has been erroneously regarded as a single disease. Such error in diagnosis could prevent oncologists from using specific or specialized treatment regimen which could improve patient survival.

As explained before, high-grade serous ovarian cancers constitute majority (~80%) of the reported cases of ovarian cancer. In these cases, the diagnosis is generally done at an advanced stage due to lack of specific clinical symptoms in the earlier stages. At such a

stage, tumor cells seed the peritoneal cavity extensively and there is an accumulation of fluid called ascites in the peritoneum, which is accompanied with abdominal pain (Ahmed and Stenvers, 2013). Since these cancers grow rapidly and metastasize easily through ascites accumulation, they have a very aggressive disease course. There are very high relapse rates and the recurring tumors are often chemoresistant, rendering the treatment regimen ineffective.

Current Treatment Strategies

The current treatment strategies include an aggressive cytoreductive or tumor debulking surgery followed by adjuvant or post-operative chemotherapy that combines platinum (e.g. use of carboplatin) and a taxane (such as taxol) (Armstrong et al., 2006). The chemotherapy also helps with management of ascites. However, as cancer develops chemoresistance and recurrence, handling large volumes of ascites becomes difficult. Alternatively, in many countries including India, the patient is administered with neoadjuvant or pre-operative chemotherapy that is expected to reduce the tumor burden before the cytoreductive surgery.

Both the strategies have been equally ineffective in improving the success rate of the treatment of ovarian cancer. Most of the cases of ovarian cancer are diagnosed at an advanced stage at which the 5-year survival rate is a mere 29% (Siegel et al., 2017). This clearly indicates that both the treatment strategies are ineffective against the advanced stage tumor since the cancer quickly relapses with chemoresistance. Therefore, there is a dire need for improvement in early detection strategies for ovarian cancer and better therapeutics that are effective against ovarian cancer cases diagnosed at an advanced stage.

The current project would test two drugs – atovaquone, an antimalarial drug and YM155, a drug developed for treatment of solid tumors – for elucidating if the drugs works through a common mechanism because of presence of a common functional chemical group.

Drug Repurposing: A Novel Therapeutic Strategy

In recent years, drug repurposing, or application of a drug for a disease other than the one it was originally approved for, has increasingly gained consideration as a strategy for drug development against cancer (Pantziarka et al., 2014). In comparison to *de novo* drug synthesis, the major plus point of this strategy is the availability of extensive data on the pharmacokinetic properties and toxicity of the drug. As the drug has already received approval from regulatory bodies for treatment of one disease, the chances of it getting approved for use for treatment of another disease increase since its safety profile is already known. Therefore, the researchers need to only specifically investigate for side effects upon usage in the new context and can avoid much of the general toxicity studies.

Atovaquone (figure 3) is an anti-malarial drug that is FDA-approved and has been clinically available since 2000. It is sold in combination with proguanil as Malarone™ as a drug for malaria prophylaxis and treatment. It is commonly prescribed as a travel medication in the Western countries. Apart from being used as an anti-malarial drug, it is also used for the treatment of pneumocystic pneumonia (PCP), toxoplasmosis and babesiosis (in combination with

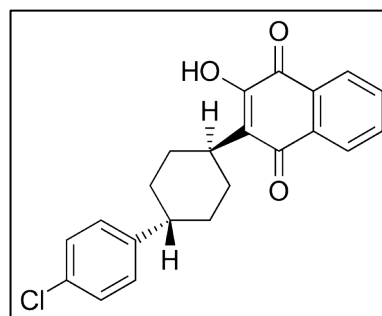


Figure 3 Chemical Structure of Atovaquone

azithromycin) (Hughes et al., 1993; Radioff et al., 1996). Atovaquone is shown to exhibit its antiparasitic action by inhibiting the mitochondrial cytochrome *bc*₁ complex or Complex III of the electron transport chain in the parasite by binding to the Qo site of the complex which leads to the collapse of mitochondrial membrane potential (Birth et al., 2014). Birth *et al*, the authors of the paper that reported this mechanism also suggest substitutions at a few places in the complex that could bring a difference in the potency of atovaquone to affect the parasite cytochrome *bc*₁ and human cytochrome *bc*₁. For example, the phenylalanine at position 278 interacts with Ile299 and its substitution to alanine in humans could destabilize the interaction of the complex with chlorophenyl ring of atovaquone. This could account for the lower potency of atovaquone in inhibiting the human cytochrome *bc*₁.

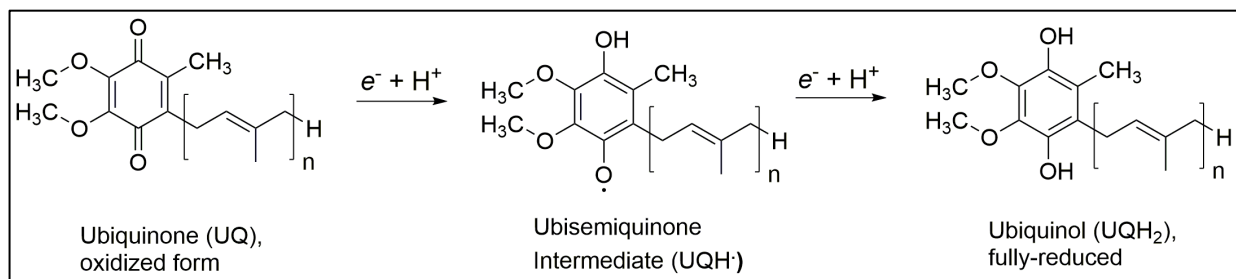


Figure 4 The three oxidative states of ubiquinone.

Chemically, atovaquone is the hydroxy-1,4-naphthoquinone analogue of ubiquinone, an important player in the electron transport chain (figure 4). Ubiquinone can exist in three redox states: ubiquinone, the fully oxidized state in which it has not accepted any electrons; ubisemiquinone – an intermediate state in which it has accepted one electron; and ubiquinol – the fully reduced state in which it has accepted two electrons. This ability of ubiquinone to reversibly function as an electron carrier is essential for its ability to transfer electrons between Complex I, II (donors) and Complex III (final acceptor). This is so because the Fe-S clusters of Complex III can accept only one electron at a time and therefore, while ubiquinone can accept two electrons at a time, it can stably maintain itself in the ubisemiquinone state and then transfer the second electron to a second Fe-S cluster, thus preventing the formation of reactive oxygen species (ROS). Atovaquone, due to high chemical structural similarity with ubiquinone, could potentially function by being its competitive inhibitor and interfere in the electron transfer between Complex I, II and Complex III. This stalling of electron flow could essentially lead to the formation of reactive oxygen species and thus induction of oxidative stress in the cell which leads to apoptosis (Guzy and Schumacker, 2006; Mather et al., 2005). Atovaquone could, therefore, be used to target human cancer cells that heavily depend on their mitochondria for energy and metabolism by being a competitive inhibitor of ubiquinone. From the existing data, it is known that atovaquone is a well-tolerated drug and it does not cause myelosuppression. Such features make atovaquone a strong candidate for drug-repurposing studies aiming for cancer chemotherapy.

YM155 (figure 5) or sepantronium bromide is a small molecule that has been shown to be safe and effective against certain subtypes of lung cancer, prostate cancer, melanoma and lymphoma in phase I/II clinical trials (Cheson et al., 2012; Giaccone et al., 2009; Satoh et al., 2009; Tolcher et al., 2008). Most of the reports till now indicate that YM155 functions by inhibiting the expression of an anti-apoptotic protein, survivin (Cheng et al., 2012; Minematsu et al., 2009; Nakahara et al., 2007). However, in recent years, there have also been reports of survivin-independent action of YM155 (Sim et al., 2017; Vequaud et al., 2015).

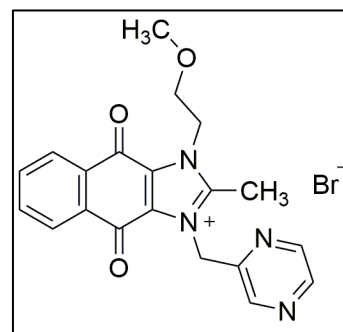


Figure 5 Chemical Structure of YM155

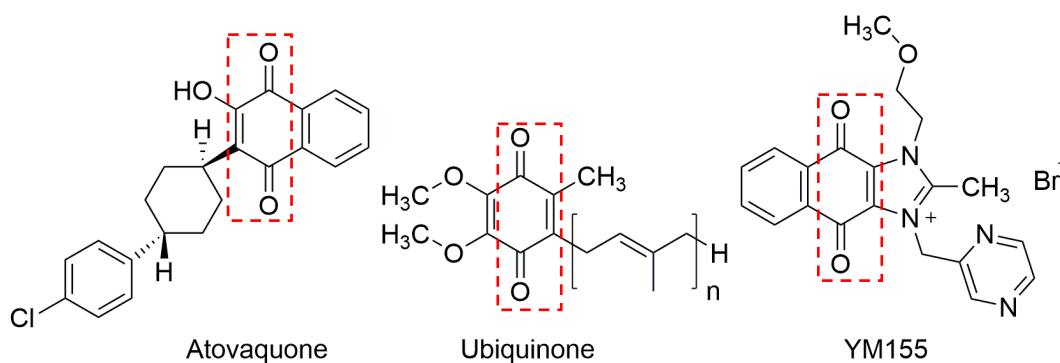


Figure 6 Structural Comparison of Atovaquone and YM155 with Ubiquinone.

The structural similarity of YM155 to ubiquinone (figure 6) suggests that its function could also be dependent on its ability to competitively inhibit electron transfer in the mitochondrial electron transport chain. Since YM155 has been reported to be safe, well-tolerated and effective against a variety of other cancers in Phase I/II clinical trials, it is included in this study for investigation of the mechanism of its anticancer action and development as a chemotherapeutic against ovarian cancer.

Atovaquone and YM155 exhibit cytotoxic activity in human ovarian cancer cell lines such as ECC-1, OVCAR3, SKOV3 and MCF-7, a breast cancer cell line (Kapur *et al*, unpublished). Specifically, both the drugs induce oxidative stress in these cell lines which is reflected in the increase in the production of ROS. This leads to induction of apoptosis in these cell lines which is abrogated upon treatment with N-acetylcysteine, which is an ROS quencher. To further develop these two drugs as chemotherapeutics against ovarian

cancer, this project aims to investigate their effectiveness in murine ovarian cancer cell lines and in *in vivo* mouse models.

Aim of the Study:

To conduct preclinical drug development studies to repurpose atovaquone and develop YM155 as chemotherapeutic agents against ovarian cancer.

Specific objectives of the study:

- i. To elucidate the mechanism of action of atovaquone and YM155 in murine ovarian cancer cell lines
- ii. To test the efficacy of the drugs in *in vivo* syngeneic mouse models
- iii. To develop adjuvant therapies that can be combined with the drugs to enhance their efficacy

Materials and Methods

- **Cell Lines and Cell Culture.** ID8 and MOSEC are cell lines that come from the ovarian surface epithelium of C57BL/6 strain of *Mus musculus* and are spontaneously transformed. The ID8 cell line is derived from a late passage clone of MOSEC that results in higher tumor burden (Roby et al., 2000). ID8 and MOSEC cell lines were obtained from Dr. Katherine Roby (University of Kansas Medical Center). The cell lines were validated by performing Single Tandem Repeat (STR) analysis (Genetica DNA Laboratories, Burlington, NC) and the cell lines were used within six months of the date of analysis. The cells were cultured in DMEM (Dulbecco's Modification of Eagle's Medium) with 4.5 g/L glucose, L-glutamine and sodium pyruvate from Corning Cellgro (Manassas, VA) substituted with 5% Fetal Bovine Serum (FBS) from Gemini Bio-Products (Sacramento, CA), 10 µg/mL Insulin, Transferrin and Selenium (ITS) from Lonza (Walkersville, MD) and 1x penicillin-streptomycin was used as medium to culture the ID8 and MOSEC cell lines. Phosphate Buffered Saline (PBS) without calcium and magnesium from Corning Cellgro (Manassas, VA) was used to wash the cells and Trypsin-EDTA solution was used to detach the adherent cells from the tissue-culture treated dishes (Corning Inc. – Life Sciences, Durham, NC).

- **Chemicals and Antibodies.** Atovaquone was purchased from Sigma Aldrich (St. Louis, MO) and YM155 was purchased from EMD Millipore (Burlington, MA). 3-(4,5-dimethylthiazol-2-yl)-2,5-diphenyl tetrazolium bromide (MTT) was purchased from Sigma (St. Louis, MO). FITC Annexin V Apoptosis Detection Kit was purchased from BD Pharmingen (San Diego, CA). Radioimmunoprecipitation assay (RIPA) buffer containing protease inhibitor cocktail, Pierce™ BCA Protein Assay Kit, SuperSignal West Dura and Femto Extended Duration Substrate were purchased from Thermo Scientific (Rockford, IL). Immobilon PVDF membrane, used for blotting was purchased from Millipore Sigma (Burlington, MA). All primary antibodies were purchased from Cell Signaling Technology (Danvers, MA) and the secondary antibodies were purchased from Jackson ImmunoResearch Laboratories (West Grove, PA), respectively. 2',7'-dichlorodihydrofluorescein diacetate (H₂DCFDA) and N-acetylcysteine (NAC) were purchased from Sigma (St. Louis, MO).
- **Cell viability assay.** The viability of cells after concentration- and time-dependent treatments with atovaquone and YM155 was monitored by the MTT assay as described previously (Denizot and Lang, 1986; Spinner, 2001). Briefly, cells were plated at a density of 1000 cells/well in 96-well plate. After 24 hours, these cells were treated with atovaquone or YM155 for 24, 48 or 72 hours followed by the addition of MTT (final concentration – 0.5 mg/ml) to each well. The plates were then incubated at 37°C for 3 hours after which the medium was removed. The purple formazan crystals were dissolved in 100 µl DMSO with brief gentle shaking. The absorbance was recorded on Spectra MAX 190 (Molecular Devices, Sunnyvale, CA) microplate reader at a wavelength of 570 nm. The graphs were plotted using GraphPad Prism 7 (La Jolla, CA) and the IC₅₀ concentration was determined using Microsoft Excel. All data points are average of eight biological replicates.
- **Apoptosis detection using Annexin V staining.** Induction of apoptosis in cells treated with atovaquone or YM155 was evaluated using flow cytometry as described in (Liu et al., 2012). Briefly, cells treated with atovaquone or YM155 for 24 h were

harvested and washed twice with PBS. 1×10^5 cells were transferred to 5 mL flow tubes and 5 μ L Annexin V-FITC and 5 μ L propidium iodide (PI) were added to label the cells. The cells were gently vortexed and incubated for 15 minutes at room temperature in dark. The cells were analyzed by flow cytometry on an Attune NxT flow cytometer (ThermoFisher Scientific, Waltham, MA) within 1 hour of labeling. The data obtained was analyzed using FlowJo software (FlowJo LLC, Ashland OR). Percentage of early (Annexin V+/propidium iodide-) and late (Annexin V+/propidium iodide+) apoptotic cells in the control and treated groups were determined. The graphs were plotted using GraphPad Prism 7 and the results are an average of three biological replicates.

- **Western blotting.** Cells (5×10^5) plated in 100 mm dishes were treated with atovaquone or YM155, washed with ice-cold PBS and lysed in RIPA buffer supplemented with protease inhibitor cocktail. Protein concentration was measured using BCA protein assay kit. 25 μ g of the protein were electrophoresed on 6-12% polyacrylamide gels, and electrophoretically transferred onto PVDF membranes. The membranes were then blocked using a solution of 5% skimmed milk in Tris-Buffered Saline with Tween 20 (TBST). After this, the membranes were incubated with the primary antibodies for either overnight or for one hour (β -actin), followed by appropriate HRP-conjugated secondary antibodies. The protein bands were visualized with chemiluminescence substrate by autoradiography. The developed autoradiography films (MidSci, St. Louis, MO) were scanned using FluorChem 8900 Imaging System (Alpha Innotech, Santa Clara, CA) and the images were processed using the ImageJ software (NCBI).
- **Detection of intracellular reactive oxygen species.** The increase in the level of intracellular reactive oxygen species upon exposure of ID8 and MOSEC cells to atovaquone and YM155 was monitored using H₂DCFDA and flow cytometry as described in (Liu et al., 2012). The cells were incubated with 10 μ M H₂DCFDA for 30 min at 37°C, followed by treatment with atovaquone or YM155 for 15 min. The cells were washed with PBS, harvested and 5 μ L PI was added to stain the dead cells. The

intensity of fluorescent 2',7'-dichlorofluorescein (DCF), obtained upon cleavage of the acetate groups by oxidation was the readout for ROS levels measured by flow cytometry on Attune NxT flow cytometer (ThermoFisher Scientific, Waltham, MA). The data obtained was analyzed using FlowJo software (Ashland, OR). The graphs were plotted using GraphPad Prism 7 and the results are an average of three biological replicates.

- **Pre-treatment of cells with N-acetylcysteine (NAC).** Cells in 6-well plates were treated with 1mM NAC for 30 min (pre-treatment) and were then washed with PBS. Afterwards, the cells were given overnight treatment with atovaquone or YM155 and then were processed to determine the level of apoptosis induction.
- **Study Approval.** Experiments performed in mice were approved by the Institute Animal Care and Use Committee (IACUC) at University of Wisconsin-Madison.
- **Effect of atovaquone on *in vivo* growth of MOSEC tumors.** Approximately 10×10^6 MOSEC cells were injected intraperitoneally into female C57BL/6 mice ($n = 5$ for each control and treatment groups). After 7 days of injection of the MOSEC cells, Mepron® (commercially available liquid suspension of atovaquone, GlaxoSmithKline) was administered to the animals by oral gavage at the final concentration of 200 mg/kg/day for 5 days a week. The body weights of animals were monitored weekly till sacrifice. The endpoint of the study was decided to be the point when animals in the control group had distended bellies due to the accumulation of ascites. Post-sacrifice, ascites fluid was collected by tapping the mice, and the disseminated tumor mass was excised from the walls of the organs surrounding the peritoneal cavity. The excised tumors were collected and weighed to determine the tumor burden in both the groups.

Results

1. Atovaquone and YM155 reduce the viability of murine ovarian cancer cell lines.

MTT assays conducted on ID8 cells showed that both atovaquone and YM155 were effective in inhibiting their proliferation at their respective IC₅₀ concentrations (25 μM for atovaquone and 25 nM for YM155) (figure 7). MOSEC cells also show similar IC₅₀ concentration for both drugs (data not shown).

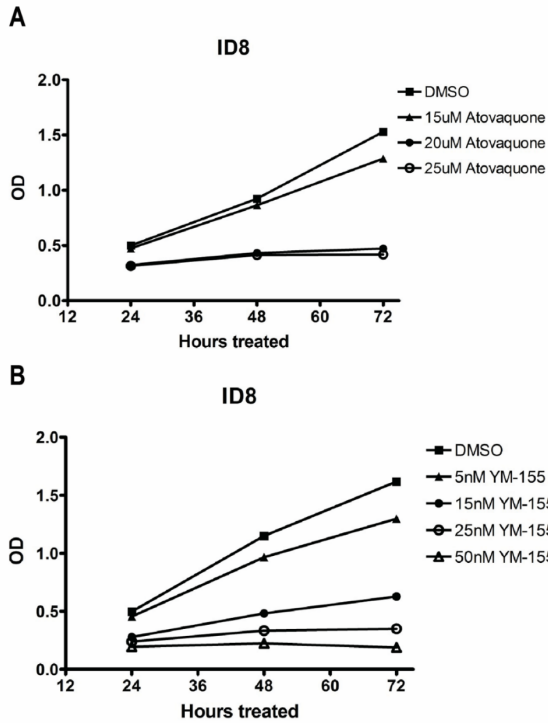


Figure 7 Cell Viability measured by MTT assay. ID8 cells were treated with different concentrations of atovaquone (A) or YM155 (B) for 24, 48 and 72 hours. The optical density (OD) decreases with increase in duration of treatment and/or concentration of the compound, indicating that treatment with the compound decreases the number of viable cells.

2. Atovaquone and YM155 cause apoptosis in murine ovarian cancer cells.

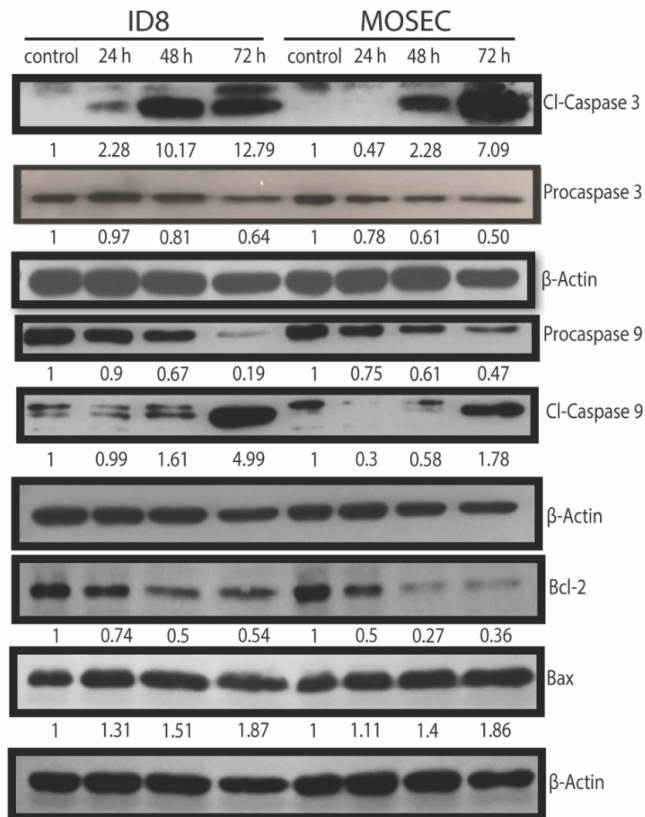


Figure 8 Atovaquone decreases the viability of cells by inducing apoptosis in ID8 and MOSEC cells. ID8 and MOSEC cells were treated with Atovaquone (25 μ M) for 24, 48 and 72h and probed for various apoptosis markers by western blotting. Procaspase 3 and procaspase 9 show a decrease in expression and correspondingly, cleaved caspase-3 and cleaved caspase 9 show an increase. The anti-apoptotic protein Bcl-2 expression decreases while

The decrease in the viability of cells treated with atovaquone and YM155, as evident from the MTT assays can be ascribed to induction of apoptosis in these cells. ID8 and MOSEC cells show a consistent decrease in procaspase 3 and procaspase 9, and, an increase in cleaved caspase 3 and cleaved caspase 9 upon treatment with atovaquone. These cells also show a decrease in the expression of anti-apoptotic protein Bcl-2 and an increase in the expression of Bax upon treatment with atovaquone (figure 8). Similarly, upon treatment with YM155, there is an increase in the expression of cleaved caspase-3 and cleaved caspase-9 with time, along with a decrease in procaspase 9. There is also a decrease in the expression of Bcl-2 and an increase in the expression of Bax (figure 9).

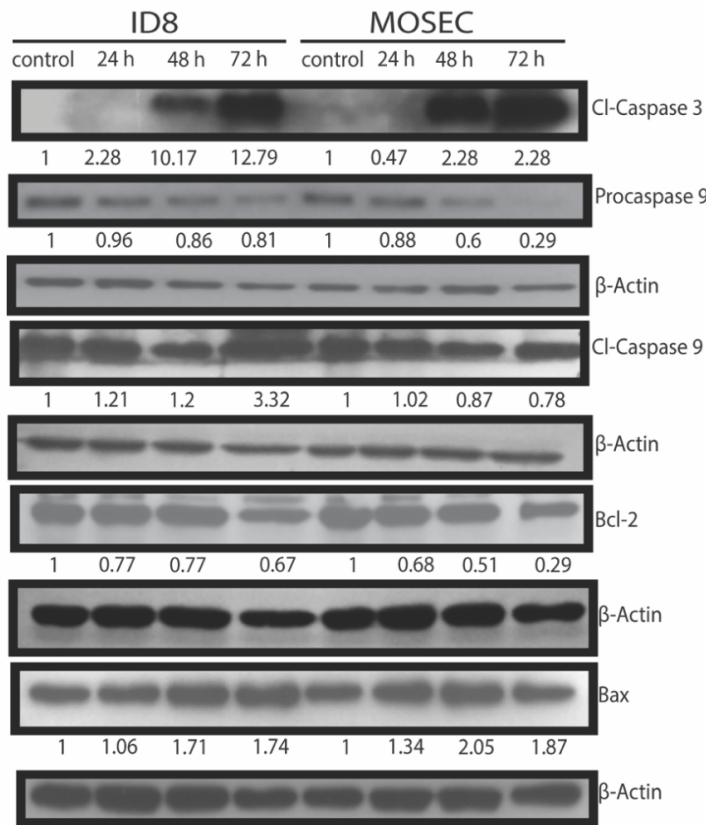


Figure 9 YM155 decreases the viability of cells by inducing apoptosis in ID8 and MOSEC cells. ID8 and MOSEC cells were treated with YM155 (25 nM) for 24, 48 and 72h and probed for various apoptosis markers by western blotting. Procaspase 9 shows a decrease in expression and correspondingly, cleaved caspase-3 and cleaved caspase 9 show an increase. The anti-apoptotic protein Bcl-2 expression decreases while the expression of pro-apoptotic protein Bax increases with time.

Induction of apoptosis was also verified by labeling atovaquone (figure 10) or YM155 (figure 11)-treated ID8 and MOSEC cells with annexin V-FITC and propidium iodide. Both the cell lines were treated with the IC₅₀ concentration of each one of the two drugs for 24 hours and then, were stained with annexin V-FITC and propidium iodide.

An increase in the population of cells upon drug treatment that are annexin-V+ indicates that there is an induction of apoptosis.

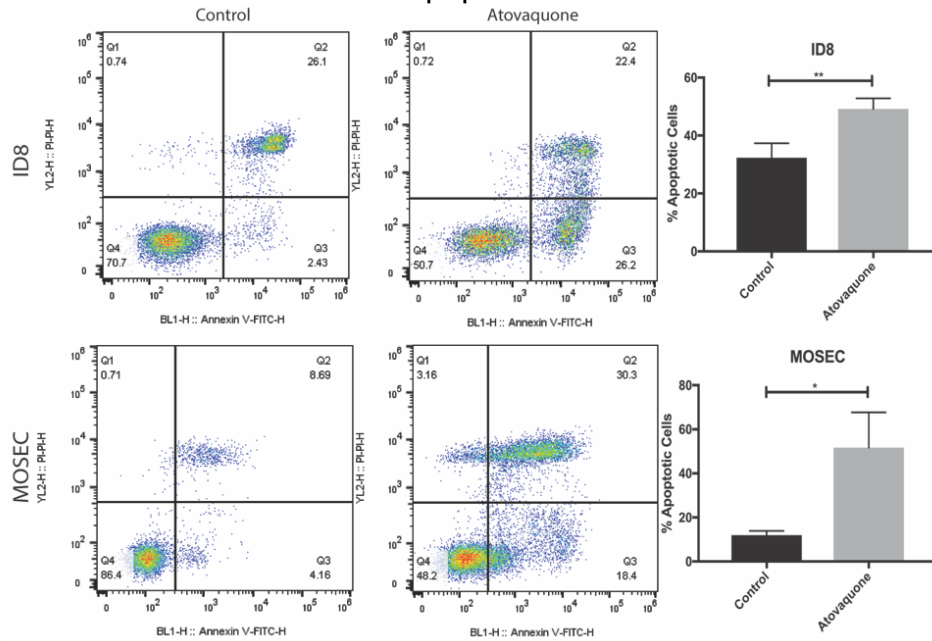


Figure 10 Annexin V-FITC and propidium iodide staining indicates that treatment with atovaquone for 24 hours induces apoptosis in ID8 and MOSEC cells. With respect to control, there is a higher fraction of cell population in the quadrants that are annexin-V positive, indicating cells in early and late apoptosis. * : $p < 0.05$, *** : $p < 0.001$

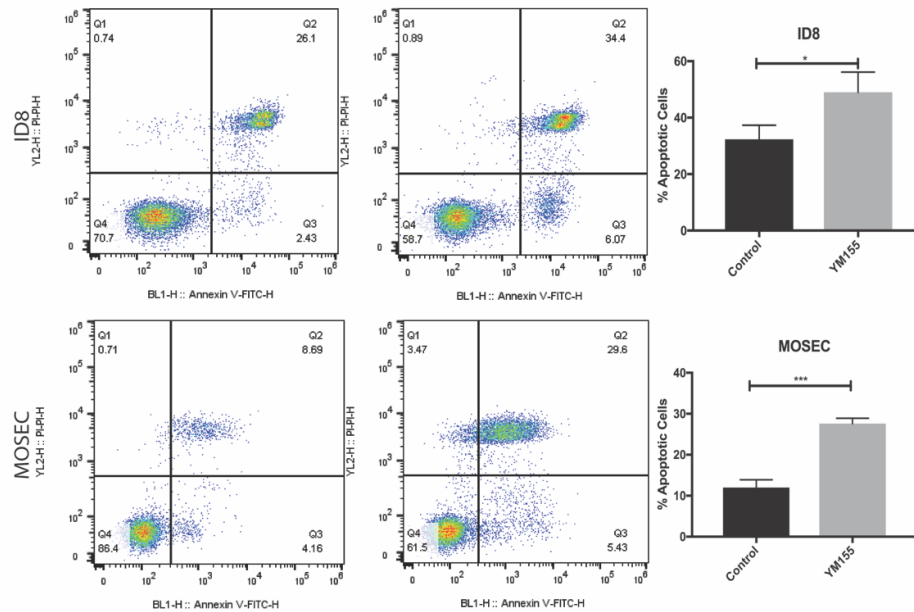


Figure 11 Annexin V-FITC and propidium iodide staining indicates that treatment with YM155 for 24 hours induces apoptosis in ID8 and MOSEC cells. With respect to control, there is a higher fraction of cell population in the quadrants that are annexin-V positive, indicating cells in early and late apoptosis. ** : $p < 0.01$, * : $p < 0.05$

3. The apoptosis induced in ID8 and MOSEC cells upon treatment with atovaquone or YM155 is caused by oxidative stress induced by the drug.

We hypothesized that treatment of ID8 and MOSEC cells with atovaquone and YM155 induces oxidative stress which is responsible for the ability of the drugs to reduce the viability of the cells and induce apoptosis. To prove that, ID8 cells were pre-treated with the N-acetylcysteine (NAC), an ROS quencher for 30min. The, the medium containing NAC was removed, and cells were washed with PBS. This step was taken to eliminate excess NAC from the medium that could reduce the drug by reducing its naphthoquinone group. The cells were then treated with atovaquone or YM155 for 24h and processed for apoptosis detection assay using annexin V. Pre-treatment with NAC significantly decreased the fraction of atovaquone- or YM155-treated cells in early and late apoptotic stages (as indicated by Annexin V staining, figure 12 and 13 respectively). This hypothesis was also supported by the observation that treatment with atovaquone induced a rapid increase in the levels of intracellular reactive oxygen species in ID8 and MOSEC cell lines. However, a significant increase was not reported in this assay upon treatment of the cells with YM155 (figure 14).

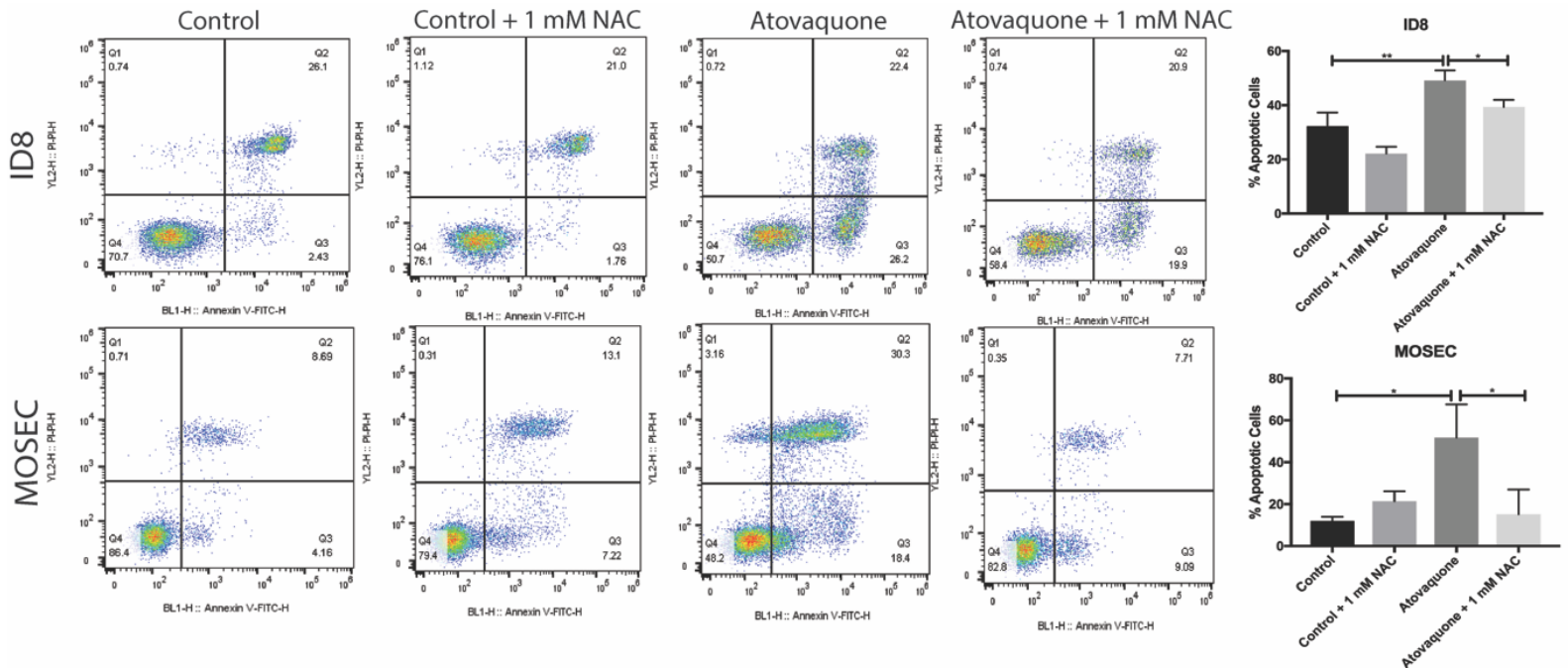


Figure 12 Oxidative stress is essential for atovaquone -induced apoptosis in ID8 and MOSEC cells. * : $p < 0.05$, ** : $p < 0.01$

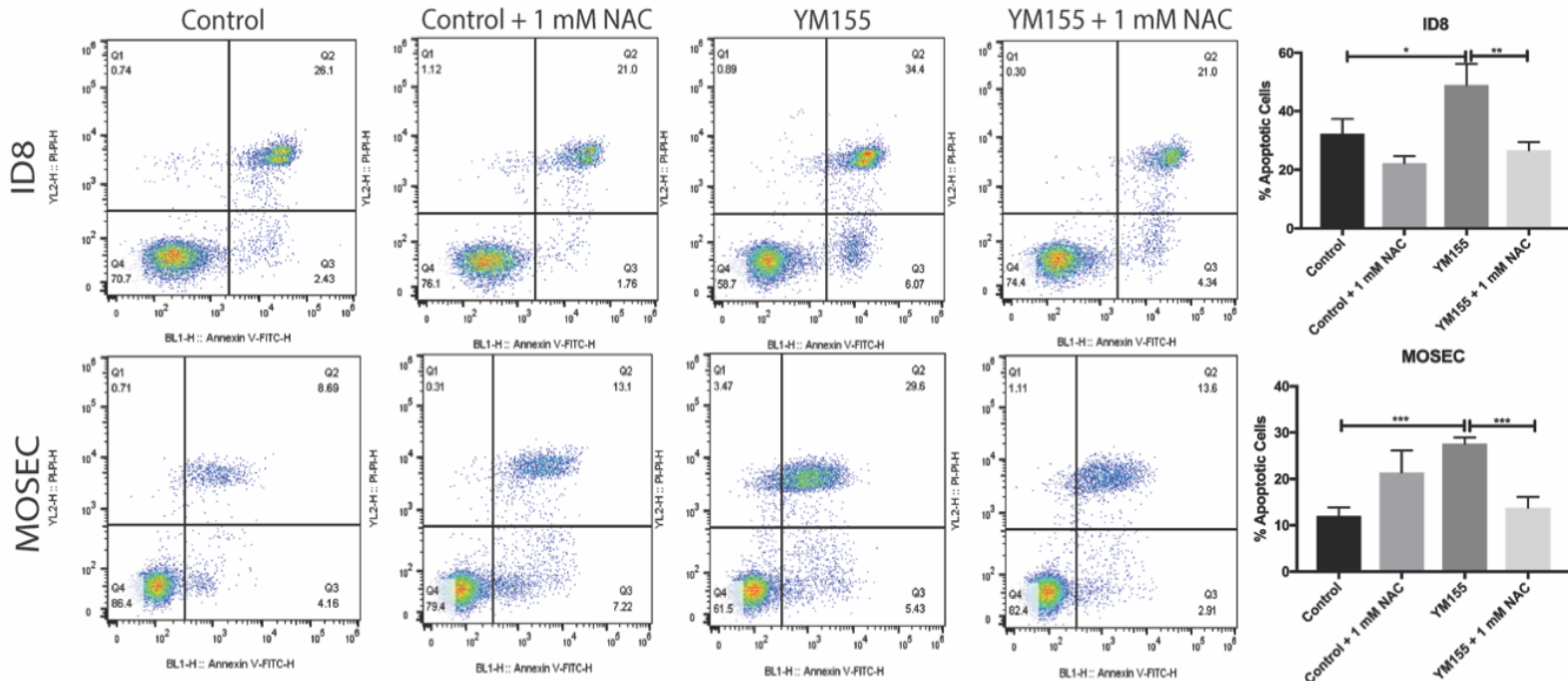


Figure 13 Oxidative stress is essential for YM155 -induced apoptosis in ID8 and MOSEC cells. * : $p < 0.05$, ** : $p < 0.01$, *** : $p < 0.001$

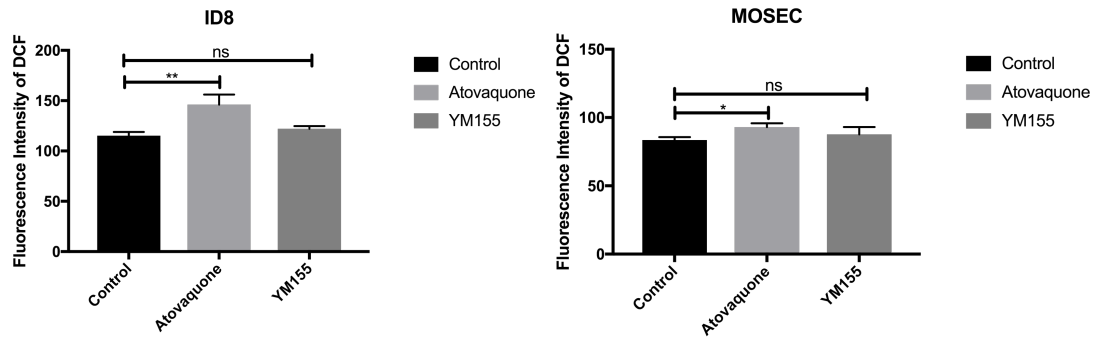


Figure 14 Treatment with Atovaquone for 15 minutes leads to a rapid increase in intracellular reactive oxygen species which is reflected by the activation of the dye H2DCF-DA.

4. Atovaquone and YM155 decrease expression of anti-apoptotic protein, *Survivin* and proliferation marker, *PCNA* and increase the expression of *p53*.

An investigation by western blotting also indicates that upon treatment with either atovaquone or YM155, there is a decrease in the expression of the anti-apoptotic protein, survivin in ID8 and MOSEC cells. This is a significant result because YM155 has been shown to be functional by primarily inhibiting survivin expression. However, since it is evident that both the drugs decrease the expression of survivin, it is possible that survivin is not the main target of YM155. Treatment with atovaquone or YM155

also decreases the expression of PCNA, which is a proliferation marker and increases the expression of p53, an important tumor suppressor (figure 15).

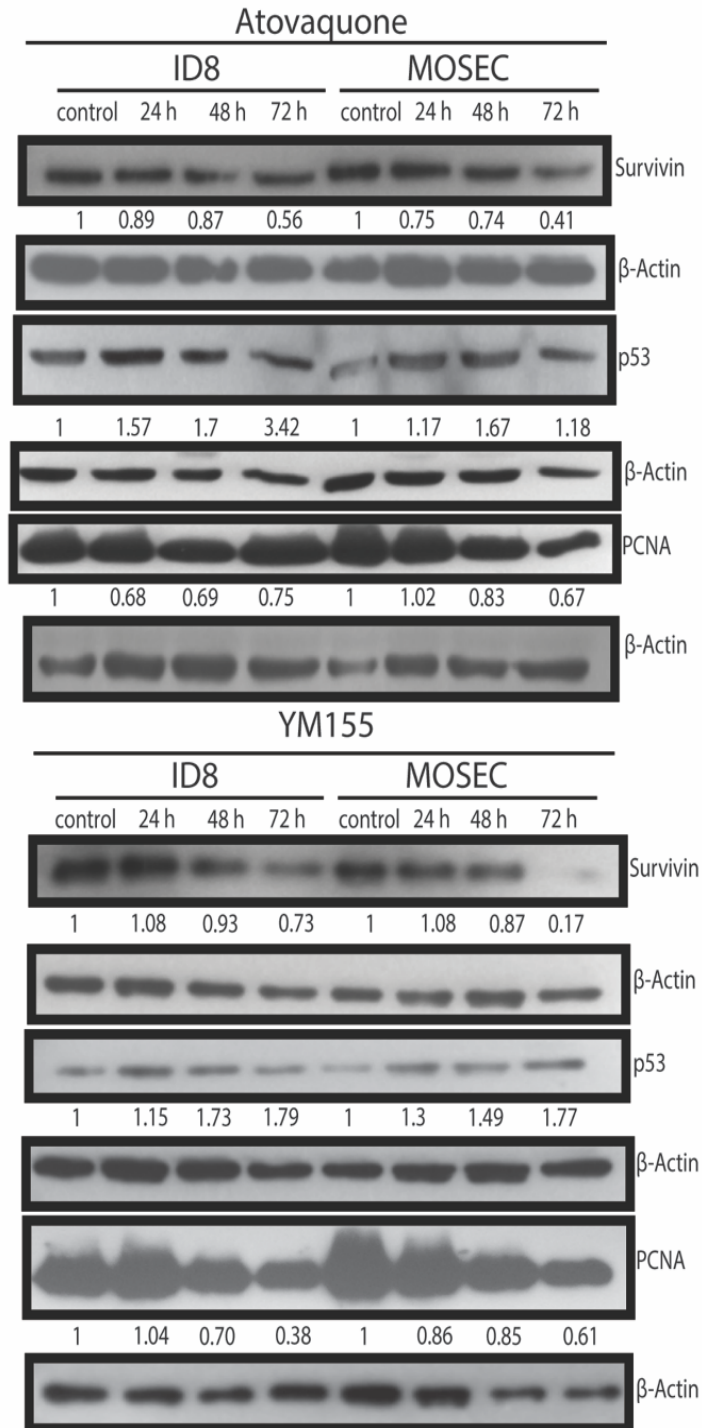


Figure 15 Treatment with atovaquone (top panel) or YM155 (bottom panel) decreases the expression of survivin (anti-apoptotic protein) and PCNA (proliferation marker), and, increases the expression of p53 (tumor suppressor).

5. Atovaquone and YM155 induce autophagy in ID8 and MOSEC cells.

Markers of autophagy, such as p62, Beclin-1 and LC3 were probed in ID8 and MOSEC cells treated with atovaquone or YM155 by western blotting. Nucleoporin 62 or p62, is sequestered in the process of autophagy, or, lack of autophagy leads to its accumulation (Bjørkøy et al., 2005). There is a clear decrease in p62 accumulation with time upon treatment of ID8 and MOSEC cells with atovaquone or YM155. Beclin-1 is also known to regulate both autophagy and apoptosis and is degraded with the induction of autophagy. As shown in the blots, treatment with atovaquone or YM155 shows a decrease in the levels of Beclin-1 with time which corresponds well with increased degradation of Beclin-1. Lastly, LC3B is a microtubule-associated protein that is ubiquitously present in the cytosol in the LC3B1 form. During autophagy, LC3B1 (the cytosolic form) is engulfed by autophagosomes and is converted to LC3B2 that is recruited to the autophagosome membrane (Tanida et al., 2008). Treatment with atovaquone or YM155 shows a decrease in the abundance of LC3B1 and an increase in LC3B2 which match well with the induction of autophagy (figure 16).

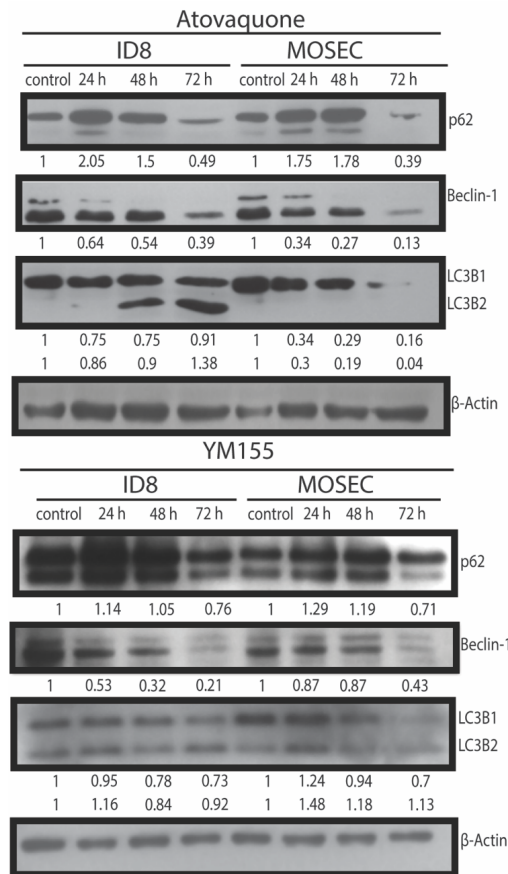


Figure 16 Treatment with atovaquone (top panel) or YM155 (bottom panel) induces autophagy in ID8 and MOSEC cells.

6. Treatment with atovaquone or YM155 increases the expression of Nrf-2.

Nrf-2 is a transcription factor that serves as the master regulator of antioxidant pathways in the cells. Treatment with atovaquone or YM155 induces a higher expression of Nrf-2 (figure 17), as it induces oxidative stress in the cells (result 3).

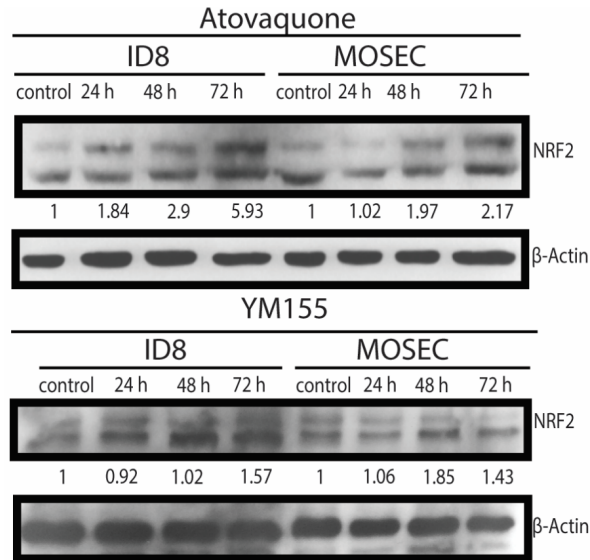


Figure 17 Treatment with atovaquone (top panel) or YM155 (bottom panel) increases expression of NRF2.

7. Oral gavage is the best delivery route for administration of atovaquone to mice.

Atovaquone is practically insoluble in water (< 1mg/ml at 25°C) but is soluble in DMSO (>10 mg/ml at 25°C) (Sigma Aldrich). However, since DMSO itself can be cytotoxic to the cells, it cannot be used as a safe drug delivery agent. Therefore, we investigated for alternative drug delivery methods and first tested the effectiveness of pluronic micelles carrying atovaquone *in vitro* by doing MTT assay on ECC1 (human ovarian cancer cell line) and ID8 cells. However, atovaquone was poorly soluble even in the preparatory reagents of the micelles. As a result, atovaquone precipitated out of the micelles in the MTT assay and the micelles were not effective at containing the volume of atovaquone required to achieve the desired concentration.

We then switched to using Mepron®, which is a commercially available suspension of atovaquone. It has micro-fine particles of atovaquone along with inactive ingredients – benzyl alcohol, flavor, poloxamer 188, purified water, saccharin sodium and xanthum gum (GlaxoSmithKline). Since it is approved for oral administration, Mepron® was administered at a dose of 200mg/kg for 5



Figure 18 Mepron®. Source: GlaxoSmithKline

days a week which is the maximum tolerated dose in humans, as approved by FDA. In Mepron®, benzyl alcohol is the main solvent. We, therefore, use it as the control for the *in vivo* experiments.

8. Treatment with Mepron® reduced ascites accumulation in mice.

As described in the methods, C57BL/6 mice (n=5 in control group and n=5 in the treatment group) were injected with 10×10^6 MOSEC cells intraperitoneally. Treatment, according to the above-mentioned dosing strategy (result 6) was started seven days post-injection. Ascites accumulation occurs at advanced stages of ovarian cancer. The mice were euthanized when mice in the control group showed visibly distended bellies due to ascites accumulation, which was also reflected in behavioral discomfort. 10 weeks post-injection, there was an increase in the weight of the mice in the control group, which can be ascribed to higher ascites accumulation in the control group (figure 19). 12 weeks post-injection, 2 mice in the control group were euthanized and then tapped to collect the ascites fluid. This explains the subsequent decrease in the average weight of the mice the week after (week 13), which recovers in week 14 and it further reinforces that the difference in the weight in the two groups is due to ascites accumulation. However, even with that decrease, the average weight of a mouse is still lower in the treatment group in

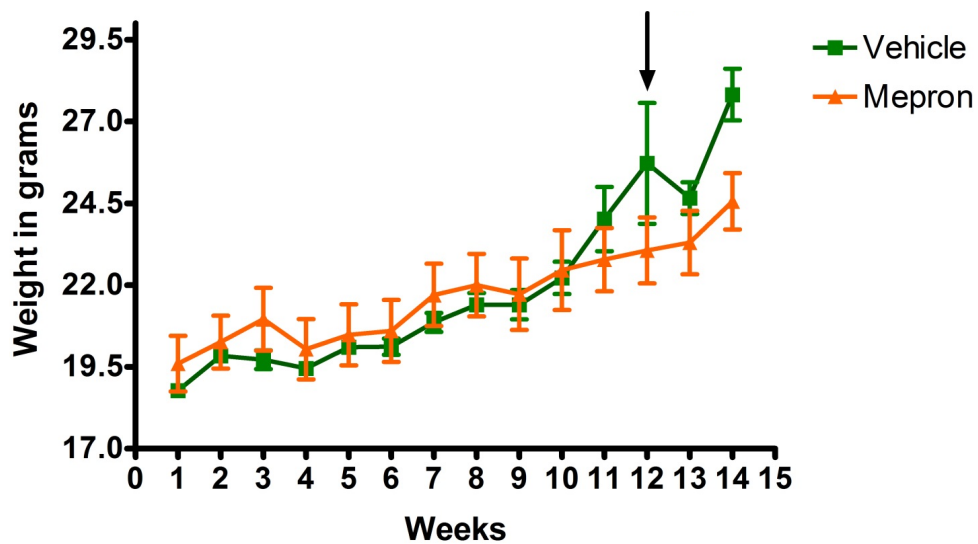


Figure 19 Treatment with Mepron® decreases ascites accumulation that is reflected in the decreased average weight of mice in the treatment group with respect to mice in the control group. The black arrow at Week 12 indicates that two mice were euthanized and tapped at week 12, two weeks before the rest of the mice were euthanized and tapped. This measure was taken since these two mice showed high amount of behavioral discomfort by Week 12.

comparison to a mouse in the control group, which indicates that the difference in the weight is due to ascites accumulation.

Treatment with Mepron® reduced ascites accumulation which is also reflected in the average volume of ascites fluid collected from mice in each group (figure 20, left) and ascites volume from individual animals in each group (figure 20, right). Mep 1 animal is an outlier in the treatment group which explains the high p-value in the graph on the left. Therefore, it can be inferred that there is a difference in the volume of ascites fluid collected from the animals in the two groups, with treatment group having the lesser volume of ascites fluid.

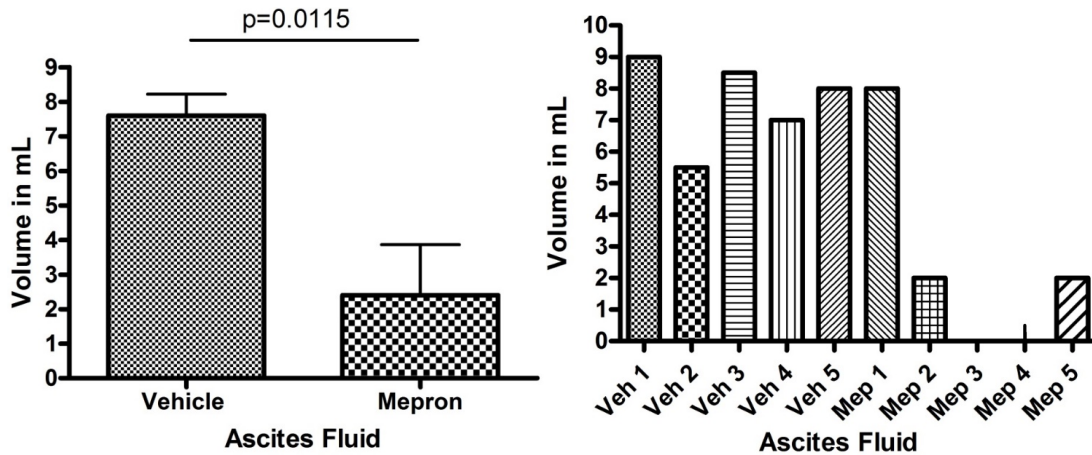


Figure 20 Treatment with Mepron® decreases ascites accumulation. The average ascites volume collected per animal is higher in the control group in comparison with the treatment group (left). The volume collected from each individual animal is shown on right.

9. Treatment with Mepron® reduced tumor burden in mice.

The effectiveness of Mepron® was also measured in terms of tumor burden. Since the MOSEC cells were given intraperitoneally, the tumors developed in a disseminated manner along the walls of the peritoneum. Upon sacrifice, all the disseminated tumor masses were excised and weighed together to measure the tumor burden. Treatment with Mepron® led to a decrease in tumor burden (figure 21).

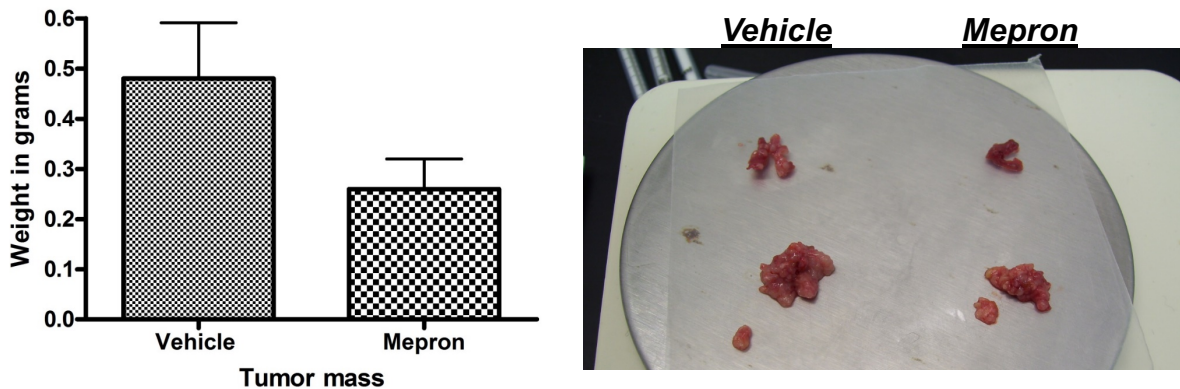


Figure 21 Treatment with Mepron® reduced the tumor burden in the mice in the treatment group (left). On the right are representative images of tumor from the walls of lung (top) and oesophageal wall (bottom). The size of tumors is visibly smaller in the treatment group. $p = 0.0112$

Discussions

In the current study, it was evident that atovaquone and YM155 reduced cell viability and induced apoptosis in mouse ovarian cancer cell lines. The drugs induced oxidative stress

in the cells which is essential for apoptosis, since quenching the reactive oxygen species using N-acetylcysteine led to a decrease in apoptosis. Treatment with atovaquone also led to a significant increase in the levels of reactive oxygen species in the cells. These results are consistent with the results previously obtained in human ovarian cancer cell lines in the Patankar lab (unpublished).

The treatment of the murine ovarian cancer cell lines with the two drugs led to a decrease in the expression of survivin, which is an anti-apoptotic protein. Almost all the existing literature on YM155 reports that YM155 functions by inhibiting the transcription of survivin gene. However, with the recent literature that survivin might not be the main target of YM155 and the result that both atovaquone and YM155 reduce the expression of survivin indicate that both the drugs target a player upstream of survivin which leads to decrease in its expression. Next, both the drugs decrease the expression of PCNA, a protein essential for proper functioning of DNA polymerase epsilon which is involved in DNA repair during replication. PCNA is thus used widely as a proliferation marker. The decrease in the levels of PCNA indicates that the drugs interfere with the cell cycle. The drugs also increase the expression of p53, a crucial tumor suppressor which is also involved in cell cycle. These preliminary results indicate that both the drugs might be affecting cell cycle at S phase by hampering DNA repair, which could lead to cell cycle arrest in S phase.

Next, the drugs also induce autophagy in both the cell lines and also increase the expression of Nrf-2. There are previous reports of YM155 inducing autophagy in cancer cells (Cheng et al., 2015; Jane et al., 2017; Vequaud et al., 2015). However, there have been no reports of atovaquone inducing autophagy in cells. Induction of autophagy could be a cell survival or cell destruction mechanism. There have been reports that link autophagy and Nrf-2 by p62. The autophagy adaptor protein p62 is reported to directly interact with Keap-1, the protein that prevents Nrf-2 from entering the nucleus and activating antioxidant pathways. There are conflicting reports of p62 upregulating Nrf-2 activation or deregulating it (Jiang et al., 2015). However, the results of this study show a simultaneous occurrence of autophagy and increase in levels of Nrf-2. Nrf-2 is the master regulator of antioxidant pathways in the cell. Since the drugs induce oxidative stress in

the cells, the cell might be activating Nrf-2 as a defense mechanism. This along with upregulation of autophagy could serve as potential chemoresistant mechanism. Therefore, studies with Nrf-2 inhibitor brusatol and autophagy inhibitors such as 3-MA and chloroquine would be essential to prove this hypothesis. These compounds could then also be used in combination with the drugs for a synergistic effect and higher efficacy.

Previous studies in the lab have shown that compounds such as citral and plumbagin which also have the α,β -unsaturated carbonyl group just like atovaquone and YM155 (figure 6) also induce apoptosis via oxidative stress (Kapur et al., 2018; Liu et al., 2012). These studies have also shown that the drugs also activate Nrf-2. Studies with plumbagin (Kapur et al., 2018) and citral, atovaquone and YM155 (unpublished) show that the compounds disrupt the mitochondrial electron transport chain which is also substantiated with molecular docking studies that show that the presence of the α,β -unsaturated carbonyl group allows these compounds to competitively interfere with ubiquinone which, as a result, delays electron transfer from ubisemiquinone and creates room for production of reactive oxygen species. It would, therefore, be important to study the role of this functional group for its ability to interfere with the electron transport chain by synthesizing analogues of atovaquone, YM155 or chemically simpler compounds that have the reduced form of the group. Validation of importance of this chemical group in the production of ROS would then allow smart drug synthesis by using this group as a starting scaffold to create compounds that functionally interfere electron transfer via ubiquinone.

Mitochondrial electron transport chain is utilized by all the cells – both normal and cancerous. Therefore, to target such a conserved pathway might lead to undesirable side effects. However, the safety of atovaquone as a drug towards normal cells is well-established. Atovaquone is a well-tolerated drug and does not cause myelosuppression. Another study has also reported that atovaquone does not induce oxidative stress in normal human fibroblast cell line (hTERT-BJ-1) and does so in MCF-7 cell line which is a breast adenocarcinoma cell line, suggesting that atovaquone as a drug is specific towards cancer cells, the mechanism of which remains unknown. Results from *in vivo* experiments in the current study provide a proof of principle that atovaquone is effective against

ovarian cancer tumors when implanted intraperitoneally to simulate the course of high-grade serous ovarian cancer as seen in human and mice. More experiments on SCID mice carrying human ovarian cancer cells or patient-derived xenografts would be essential to further establish the efficacy of the drug against ovarian cancer. These results would be essential in the design of a clinical trial that would ultimately test the effectiveness of the drug as a chemotherapeutic agent ovarian cancer.

Atovaquone is known to have poor bioavailability due to its poor solubility in polar mediums and this issue needs to be resolved by devising new vehicles. Various studies have suggested methods such as the use of nanoparticles, preparation of formulation by electron-spray ionization, etc. (Darade et al., 2018; Kate et al., 2016) However, it is yet to be studied whether these methods improve the bioavailability in the context of cancer.

Similar studies can be designed for YM155. However, in this case, YM155 can be administered differently since it is highly soluble in PBS and other safe aqueous-based solvents. Therefore, multiple modes of administration such as intravenous and intraperitoneal routes can be used instead of oral gavage to develop easier methods of drug delivery.

References

1. Ahmed, N., and Stenvers, K.L. (2013). Getting to know ovarian cancer ascites : opportunities for targeted therapy-based translational research. 3, 1–12.
2. American Cancer Society (2018). Cancer Facts and Figures 2018.
3. Armstrong, D., Bundy, B., Wenzel, L., Huang, H., Baergen, R., Lele, S., Copeland, L., Walker, J., and Burger, R. (2006). Intraperitoneal cisplatin and paclitaxel in ovarian cancer. *N. Engl. J. Med.* 353, 34–43.
4. Birth, D., Kao, W.-C., and Hunte, C. (2014). Structural analysis of atovaquone-inhibited cytochrome bc1 complex reveals the molecular basis of antimalarial drug action. *Nat. Commun.* 5, 4029.
5. Bjørkøy, G., Lamark, T., Brech, A., Outzen, H., Perander, M., Øvervatn, A., Stenmark, H., and Johansen, T. (2005). p62/SQSTM1 forms protein aggregates

degraded by autophagy and has a protective effect on huntingtin-induced cell death. *J. Cell Biol.* 171, 603–614.

6. Cheng, Q., Ling, X., Haller, A., Nakahara, T., Yamanaka, K., Kita, A., Koutoku, H., Takeuchi, M., Brattain, M.G., and Li Dr., F. (2012). Suppression of survivin promoter activity by YM155 involves disruption of Sp1-DNA interaction in the survivin core promoter. *Int. J. Biochem. Mol. Biol.* 3, 179–197.
7. Cheng, S.M., Chang, Y.C., Liu, C.Y., Lee, J.Y.C., Chan, H.H., Kuo, C.W., Lin, K.Y., Tsai, S.L., Chen, S.H., Li, C.F., et al. (2015). YM155 down-regulates survivin and XIAP, modulates autophagy and induces autophagy-dependent DNA damage in breast cancer cells. *Br. J. Pharmacol.* 172, 214–234.
8. Cheson, B.D., Bartlett, N.L., Vose, J.M., Lopez-Hernandez, A., Seiz, A.L., Keating, A.T., and Shamsili, S. (2012). A phase II study of the survivin suppressant YM155 in patients with refractory diffuse large B-cell lymphoma. *Cancer* 118, 3128–3134.
9. Darade, A., Pathak, S., Sharma, S., and Patravale, V. (2018). Atovaquone oral bioavailability enhancement using electrospraying technology. *Eur. J. Pharm. Sci.* 111, 195–204.
10. Denizot, F., and Lang, R. (1986). Rapid colorimetric assay for cell growth and survival. Modifications to the tetrazolium dye procedure giving improved sensitivity and reliability. *J. Immunol. Methods* 89, 271–277.
11. DeVita, V.T., and Rosenberg, S.A. (2012). Two Hundred Years of Cancer Research. *N. Engl. J. Med.* 366, 2207–2214.
12. Giaccone, G., Zatloukal, P., Roubec, J., Floor, K., Musil, J., Kuta, M., Van Klaveren, R.J., Chaudhary, S., Gunther, A., and Shamsili, S. (2009). Multicenter phase II trial of YM155, a small-molecule suppressor of survivin, in patients with advanced, refractory, non-small-cell lung cancer. *J. Clin. Oncol.* 27, 4481–4486.
13. Guzy, R.D., and Schumacker, P.T. (2006). Oxygen sensing by mitochondria at complex III: The paradox of increased reactive oxygen species during hypoxia. *Exp. Physiol.* 91, 807–819.
14. Howlader N, Noone AM, Krapcho M, Miller D, Bishop K, Kosary CL, Yu M, Ruhl J, Tatalovich Z, Mariotto A, Lewis DR, Chen HS, Feuer EJ, C.K. (eds) (2017). SEER Cancer Statistics Review, 1975–2014 (Bethesda).

15. Hughes, W., Leung, G., Kramer, F., Bozzette, S.A., Safrin, S., Frame, P., Clumeck, N., Masur, H., Lancaster, D., Chan, C., et al. (1993). Comparison of atovaquone(566C80) with trimethoprim-sulfamethoxazole to treat pneumocystis carinii pneumonia in patients with AIDS. *N. Engl. J. Med.* 328, 1521–1527.
16. Jane, E.P., Premkumar, D.R., Sutera, P.A., Cavaleri, J.M., and Pollack, I.F. (2017). Survivin inhibitor YM155 induces mitochondrial dysfunction, autophagy, DNA damage and apoptosis in Bcl-xL silenced glioma cell lines. *Mol. Carcinog.* 56, 1251–1265.
17. Jiang, T., Harder, B., Rojo De La Vega, M., Wong, P.K., Chapman, E., and Zhang, D.D. (2015). P62 links autophagy and Nrf2 signaling. *Free Radic. Biol. Med.* 88, 199–204.
18. Kapur, A., Beres, T., Rathi, K., Nayak, A.P., Czarnecki, A., Felder, M., Gillette, A., Ericksen, S.S., Sampene, E., Skala, M.C., et al. (2018). Oxidative stress via inhibition of the mitochondrial electron transport and Nrf-2-mediated anti-oxidative response regulate the cytotoxic activity of plumbagin. *Sci. Rep.* 8, 1073.
19. Kate, L., Gokarna, V., Borhade, V., Prabhu, P., Deshpande, V., Pathak, S., Sharma, S., and Patravale, V. (2016). Bioavailability enhancement of atovaquone using hot melt extrusion technology. *Eur. J. Pharm. Sci.* 86, 103–114.
20. Kipps, E., Tan, D.S.P., and Kaye, S.B. (2013). Meeting the challenge of ascites in ovarian cancer: new avenues for therapy and research. *Nat. Rev. Cancer* 13, 273–282.
21. Kurman, R., and Shih, I. (2010). The Origin and pathogenesis of epithelial ovarian cancer-a proposed unifying theory. *Am. J. Surg. Pathol.* 34, 433–443.
22. Kurman, R.J., and Shih, I.-M. (2016). The Dualistic Model of Ovarian Carcinogenesis. *Am. J. Pathol.* 186, 733–747.
23. Lengyel, E. (2010). Ovarian Cancer Development and Metastasis. *Am. J. Pathol.* 177, 1053–1064.
24. Liu, Y., Whelan, R., Pattnaik, B., Ludwig, K., Subudhi, E., Rowland, H., Claussen, N., Zucker, N., Uppal, S., Kushner, D., et al. (2012). Terpenoids from *Zingiber officinale* (Ginger) induce apoptosis in endometrial cancer cells through the activation of p53. *PLoS One* 7.

25. Mather, M.W., Darrouzet, E., Valkova-Valchanova, M., Cooley, J.W., McIntosh, M.T., Daldal, F., and Vaidya, A.B. (2005). Uncovering the molecular mode of action of the antimalarial drug atovaquone using a bacterial system. *J. Biol. Chem.* 280, 27458–27465.
26. Minematsu, T., Iwai, M., Sugimoto, K., Shirai, N., Nakahara, T., Usui, T., and Kamimura, H. (2009). Carrier-mediated uptake of 1-(2-methoxyethyl)-2-methyl-4,9-dioxo-3-(pyrazin-2-ylmethyl)-4,9-dihydro-1H-naphtho[2,3-d]imidazolium Bromide (YM155 monobromide), a novel small-molecule survivin suppressant, into human solid tumor and lymphoma cells. *Drug Metab. Dispos.* 37, 619–628.
27. Nakahara, T., Takeuchi, M., Kinoyama, I., Minematsu, T., Shirasuna, K., Matsuhisa, A., Kita, A., Tominaga, F., Yamanaka, K., Kudoh, M., et al. (2007). YM155, a novel small-molecule survivin suppressant, induces regression of established human hormone-refractory prostate tumor xenografts. *Cancer Res.* 67, 8014–8021.
28. NICPR (2018). Cancer Factsheet.
29. Pantziarka, P., Bouche, G., Meheus, L., Sukhatme, V., and Sukhatme, V.P. (2014). The Repurposing Drugs in Oncology (ReDO) Project. *Ecancermedicalscience* 8, 1–13.
30. Radioff, P.D., Philipps, J., Nkeyi, M., Hutchinson, D., and Kremsner, P.G. (1996). Atovaquone and proguanil for *Plasmodium falciparum* malaria. *Lancet* 347, 1511–1514.
31. Roby, K.F., Taylor, C.C., Sweetwood, J.P., Cheng, Y., Pace, J.L., Tawfik, O., Persons, D.L., Smith, P.G., and Terranova, P.F. (2000). Development of a syngeneic mouse model for events related to ovarian cancer. *Carcinogenesis* 21, 585–591.
32. Satoh, T., Okamoto, I., Miyazaki, M., Morinaga, R., Tsuya, A., Hasegawa, Y., Terashima, M., Ueda, S., Fukuoka, M., Ariyoshi, Y., et al. (2009). Phase I study of YM155, a novel survivin suppressant, in patients with advanced solid tumors. *Clin. Cancer Res.* 15, 3872–3880.
33. Seidman, J.D., Horkayne-Szakaly, I., Haiba, M., Boice, C.R., Kurman, R.J., and Ronnett, B.M. (2004). The histologic type and stage distribution of ovarian carcinomas of surface epithelial origin. *Int. J. Gynecol. Pathol.* 23, 41–44.

34. Siegel, R.L., Miller, K.D., and Jemal, A. (2017). Cancer Statistics, 2017. *CA Cancer J. Clin.* 67, 7–30.
35. Sim, M.Y., Huynh, H., Go, M.L., Yuen, J.S.P., Choe, T., and An, S. (2017). Action of YM155 on clear cell renal cell carcinoma does not depend on survivin expression levels. *PLoS One* 12, e0178168.
36. Spinner, D.M. (2001). MTT Growth Assays in Ovarian Cancer. *Methods Mol Med* 39, 175–177.
37. Stewart, B., and Wild, C. (2014). World cancer report 2014.
38. Tanida, I., Ueno, T., and Kominami, E. (2008). LC3 and autophagy. *Methods Mol. Biol.* 445, 77–88.
39. Tolcher, A.W., Mita, A., Lewis, L.D., Garrett, C.R., Till, E., Daud, A.I., Patnaik, A., Papadopoulos, K., Takimoto, C., Bartels, P., et al. (2008). Phase I and pharmacokinetic study of YM155, a small-molecule inhibitor of survivin. *J. Clin. Oncol.* 26, 5198–5203.
40. Vequaud, E., Seveno, C., Loussouarn, D., Engelhart, L., Campone, M., Juin, P., and Barille-Nion, S. (2015). YM155 potently triggers cell death in breast cancer cells through an autophagy-NF-kB network. *Oncotarget* 6, 13476–13486.
41. WHO (2018). Cancer Fact sheet.